Structure, Volume *27*

Supplemental Information

Autoinhibition Mechanism of the Ubiquitin-Conjugating Enzyme UBE2S by Autoubiquitination

Anna K.L. Liess, Alena Kucerova, Kristian Schweimer, Lu Yu, Theodoros I. Roumeliotis, Mathias Diebold, Olexandr Dybkov, Christoph Sotriffer, Henning Urlaub, Jyoti S. Choudhary, Jörg Mansfeld, and Sonja Lorenz

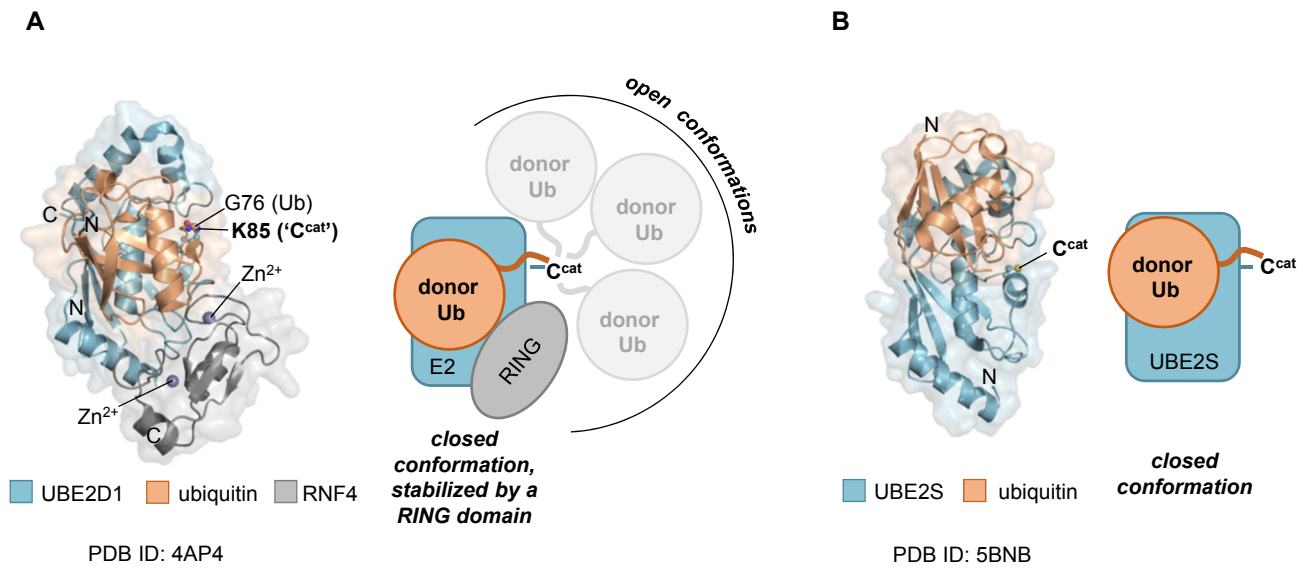

Fig S1. Conformational space of E2-linked donor ubiquitin *(related to Fig 4)*

(A) Crystal structure and accompanying cartoon model of a ternary complex of UBE2D1, donor ubiquitin, and the RING domain of RNF4 (extracted from PDB ID: 4AP4 (Plechanovová et al., 2012); note that the RING domain dimerizes, but only one monomer is displayed here). In this complex, the C-terminus of the donor ubiquitin is isopeptide-linked to an engineered lysine (K85) in lieu of the catalytic cysteine ('C^{cat}'). The RING domain stabilizes the donor in a closed conformation, as opposed to open states with no significant interface between ubiquitin and the E2. The structure is shown in a combined cartoon and surface representation; the side chain of K85 (UBE2D1) and main chain of G76 (Ub) in ball-and-stick mode. (B) Analogous representations of the closed state of a complex of $UBE2S^{UBC}$ with ubiquitin (extracted from PDB ID: 5BNB (Lorenz et al., 2016)). In this complex the ubiquitin (G76C variant) is disulfide-linked to the catalytic cysteine of UBE2S; in the crystal, however, the closed interface is formed between neighboring molecules in *trans*. Therefore, the C-terminal tail of ubiquitin (residues 73-76) is not displayed here.

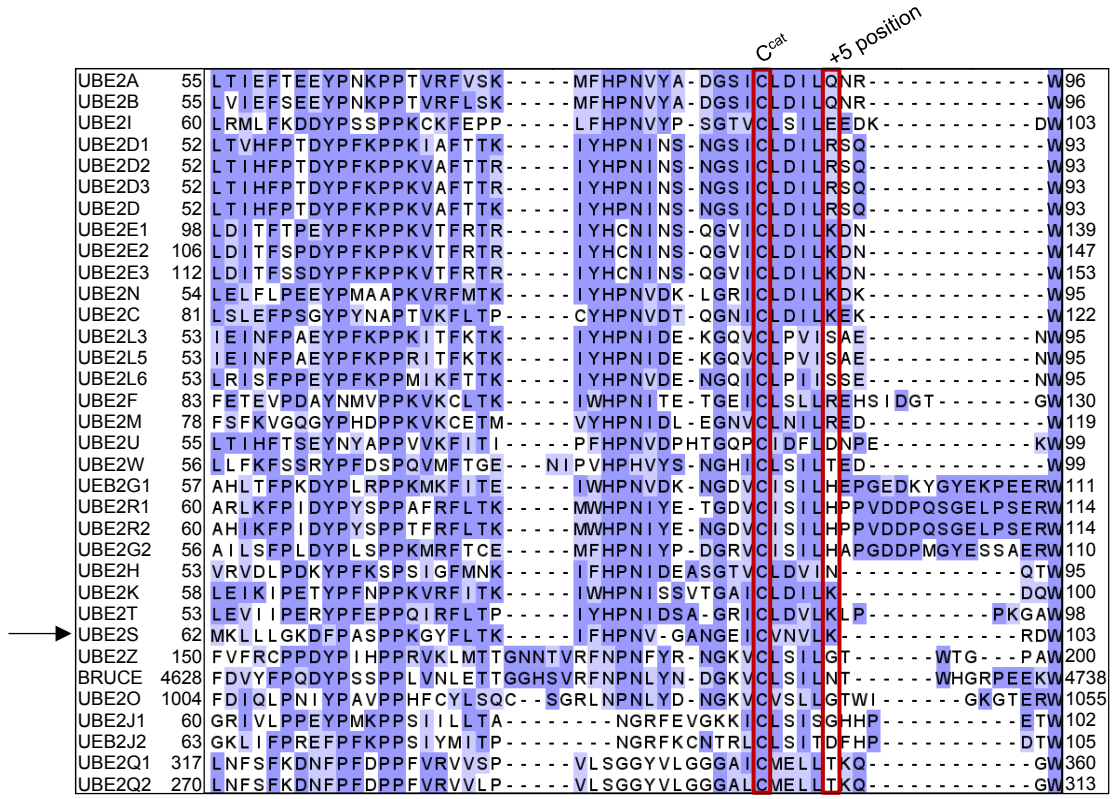

Fig S2. Lys^{+5} is conserved in ~25 % of the human E2s *(related to Table 1)*.
Sequence alignment of 34 human E2s, focusing on a ~40-residue stretch that comprises the active site. The list was compiled based on the HUGO Gene Nomenclature Committee (HGNC) (Yates et al., 2017), excluding pseudogenes and E2-like proteins that lack a catalytic cysteine residue (UBE2V1, UBE2V2, AKTIP). The amino acid sequences were extracted from UniProt (UniProt Consortium, 2018), aligned with Clustal Omega (McWilliam et al., 2013), illustrated with JalView (Waterhouse et al., 2009), and colored according to the Blosum62 score (Henikoff and Henikoff, 1992). The catalytic cysteine and the +5 position are highlighted.

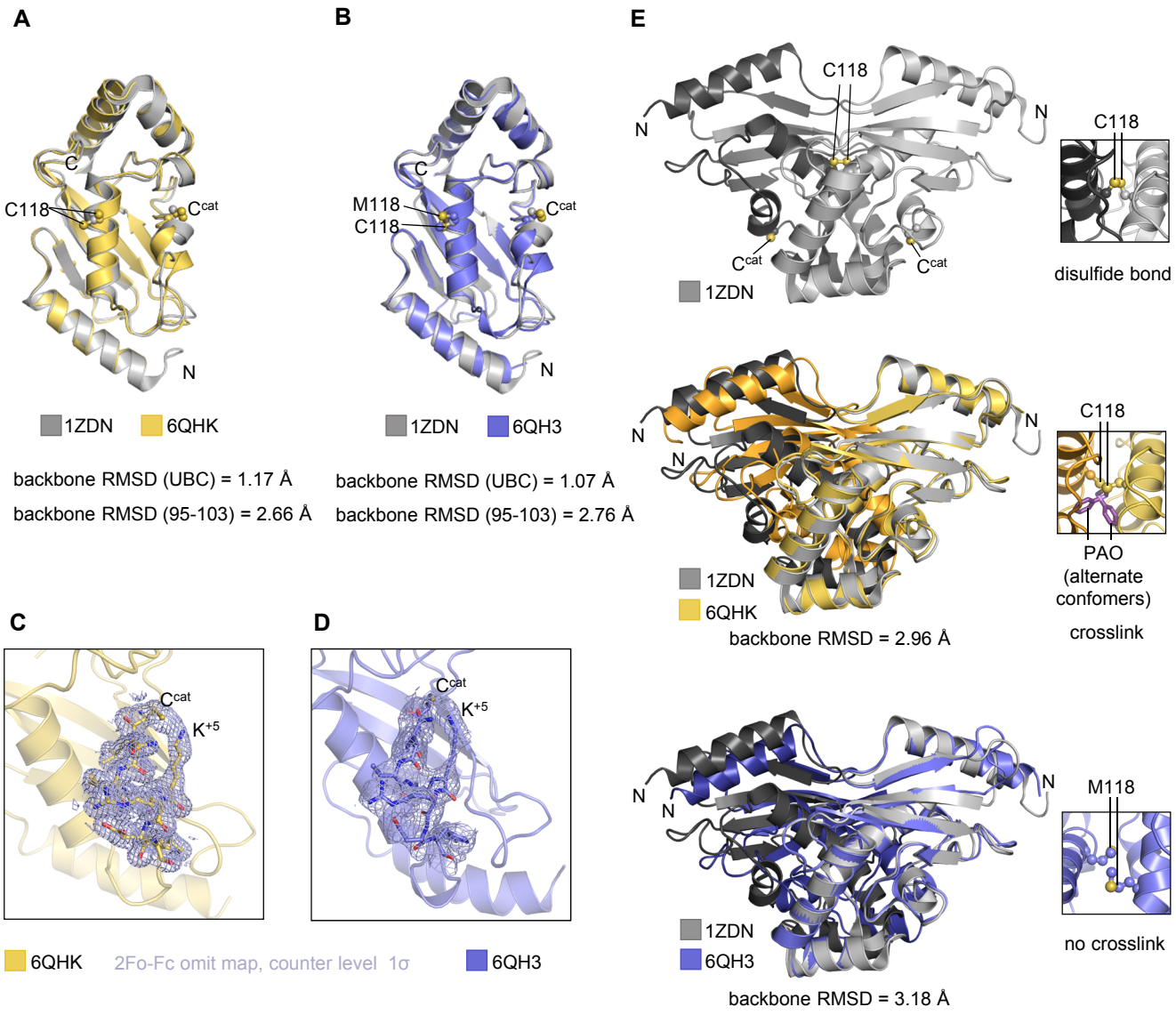

Fig S3. Comparative analysis of three crystal structures of UBE2S^{UBC} *(related to Fig 1A-C)*.
(A) Superposition of two crystal structures of UBE2S^{UBC} WT (PDB ID: 1ZDN, grey (Sheng et al., 2012) and 6QHK, yellow). Backbone RMSDs are given for the entire chain and the active-site region (residues 95-103), as calculated with CPPTRAJ: Trajectory Analysis, V18.01 (Roe and Thomas E Cheatham, 2013). (B) Superposition of the UBE2S^{UBC} WT structure (1ZDN, grey) with that of the C118M variant (6QH3, blue) and respective backbone RMSDs, calculated as in (A). (C) 2Fo-Fc omit map, countered at 1 σ, for the active-site region (residues 95-103) in the structure 6QHK. (D) Analogous 2Fo-Fc omit map for the active-site region in 6QH3. (E) Crystallographic dimers of UBE2S^{UBC} seen in 1ZDN (top), 6QHK (middle, superposed with 1ZDN), and 6QH3 (bottom, superposed with 1ZDN). The inset shows residue 118 at the subunit interface. 1ZDN has the native cysteine at position 118, which forms an inter-subunit disulfide bond; in 6QHK, a covalent crosslinker (phenylarsine oxide, 'PAO') connects the two cysteine residues and adopts two alternative conformations; 6QHK has a methionine at position 118 and thus no covalent inter-subunit linkage.

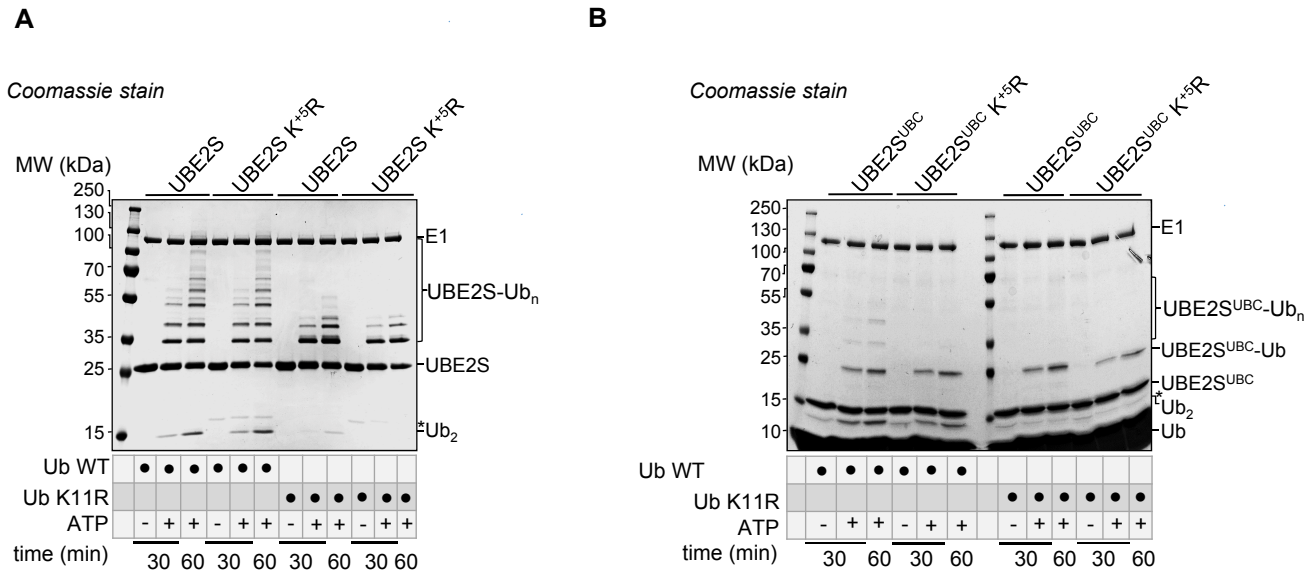

Fig S4. Impact of Lys^{+5} on ubiquitin chain formation by UBE2S and UBE2S^{UBC} ***(related to Fig 2)***

(A) Comparison of the isopeptide bond formation activities of UBE2S WT and K^{+5}R towards ubiquitin WT and K11R, respectively, *in vitro*. (B) Analogous reactions as shown in (A) using the UBE2S^{UBC} construct. In (A) and (B) auto-ubiquitinated UBE2S ('UBE2S-Ub$_n$' or 'UBE2S^{UBC}-Ub$_n$') and di-ubiquitin ('Ub$_2$') were monitored by SDS-PAGE and Coomassie staining at two time points, as indicated. The asterisks indicate a contaminant, which runs at the same height as Ub$_2$ in (B).

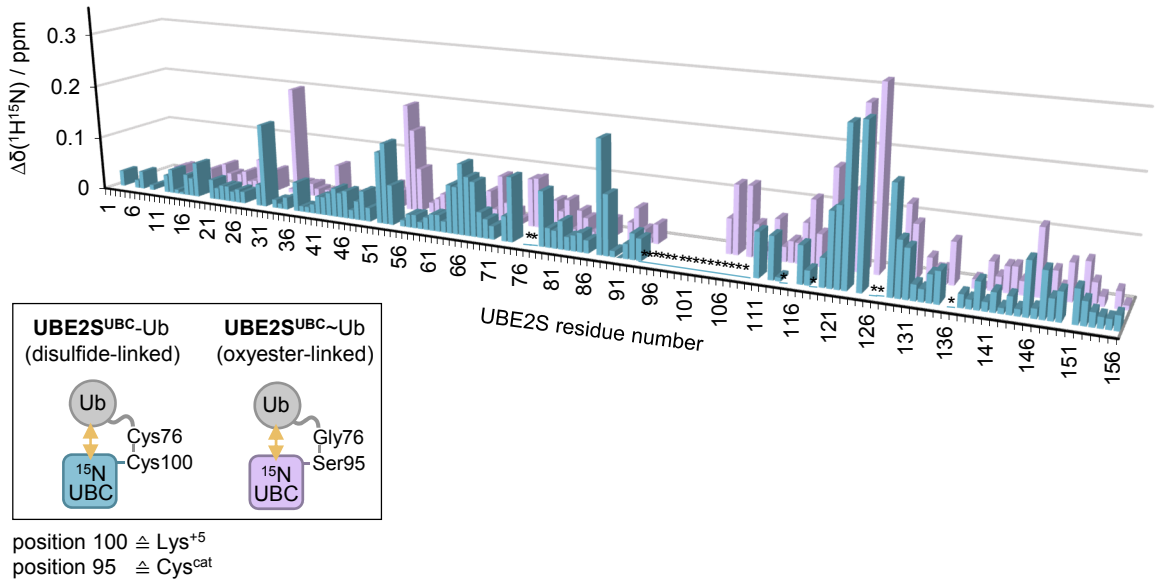

Fig S5. Active site-linked ubiquitin and Lys^{+5}-linked ubiquitin interact with UBE2S in a similar manner *(related to Fig 4)*.

Comparison of weighted, combined chemical shift perturbations, $\Delta\delta(^{1}H^{15}N)$, plotted over the residue number of UBE2S, in the context of two distinct UBE2S^{UBC}-ubiquitin conjugates. One (blue) is the disulfide-linked complex studied in Fig 4, in which ubiquitin is attached to position +5. The other (green) has ubiquitin attached to the active-site position as an oxyester (C^{cat} replaced by serine, C95S), as studied previously (Wickliffe et al., 2011). Residues labeled with an asterisk show line broadening, due to chemical exchange on an intermediate chemical shift timescale. Gaps are due to prolines (residues 9, 10, 27, 28, 35, 50, 54, 71, 74, 75, and 86) or missing assignments (residues 93 to 102 in UBE2S^{UBC} C95S; residues 3, 4, 7, 11, 18, 19, 31, 90, 111, 115, 135, and 150 in UBE2S^{UBC} (C95S/K100C/C118M)-Ub; for details, see STAR Methods).

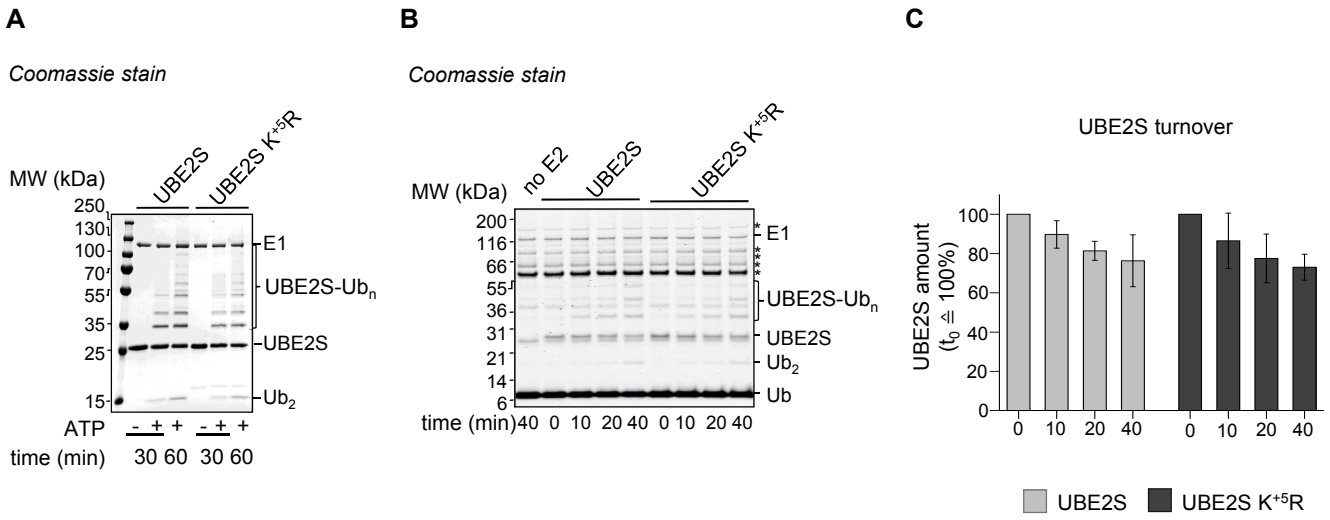

Fig S6. Coomassie-stained images of *in vitro* ubiquitination assays with UBE2S WT and K^{+5}R *(related to Fig 5)*

(A) Coomassie-stained image of the gel for which a fluorescence-based image is shown in Fig 5A. This image and data from two further experiments were used for the quantification provided in Fig 5B. (B) Coomassie-stained image of the gel for which a fluorescence-based image is shown in Fig 5C. Reaction supplements and impurities are labeled with asterisks (C) Quantification of unmodified UBE2S from (B) (as an inverse measure of UBE2S ubiquitination) relative to the input amount (determined at t_0). The mean and SDs from three independent experiments were plotted.

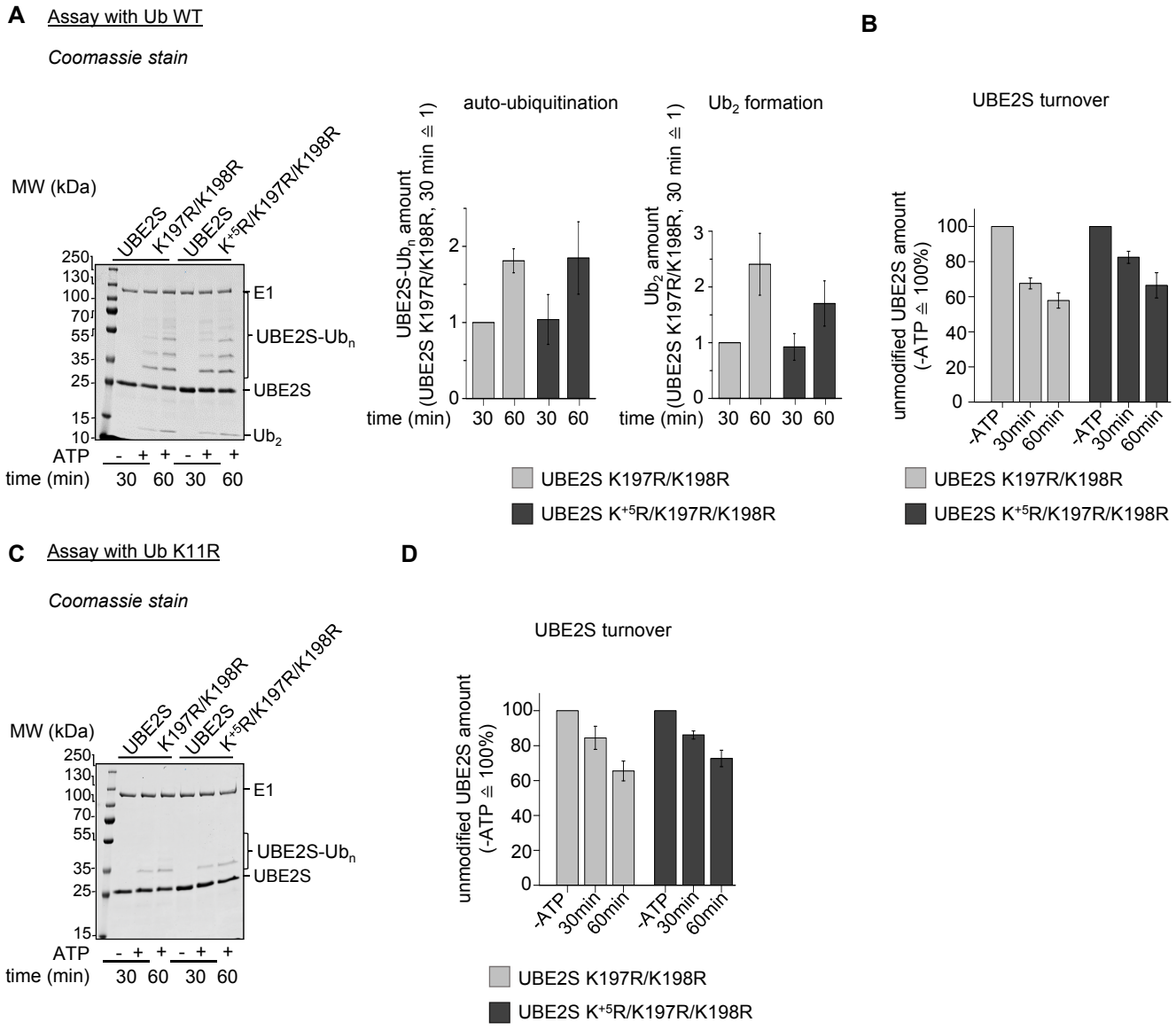

Fig S7: Impact of Lys197 and Lys198 on ubiquitin chain formation by UBE2S in E3-independent reactions *in vitro (related to Fig 5A, B)*

(A) Comparison of the isopeptide bond formation activities of UBE2S K197R/K198R and K^{+5}R/K197R/K198R towards ubiquitin WT *in vitro*. Auto-ubiquitinated UBE2S ('UBE2S-Ub_n') and di-ubiquitin ('Ub_2') were monitored by SDS-PAGE and Coomassie staining at two time points, as indicated (left). Quantification of auto-ubiquitination of UBE2S (middle) and Ub_2 formation (right), with the mean and SDs from three independent experiments plotted. The amounts of reaction products formed by UBE2S K197R/K198R after 30 minutes were set to 1. (B) Quantification of UBE2S turnover from 3 independent experiments (as shown in (A)), normalized to the amount of input enzyme ('minus ATP' lane set to 100%). (C) Comparison of the isopeptide bond formation activities of UBE2S K197R/K198R and K^{+5}R/K197R/K198R in E3-independenttowards ubiquitin K11R *in vitro*. (D) Quantification of UBE2S turnover from three independent experiments (as shown in C), with the mean and SDs plotted.

Figure S8

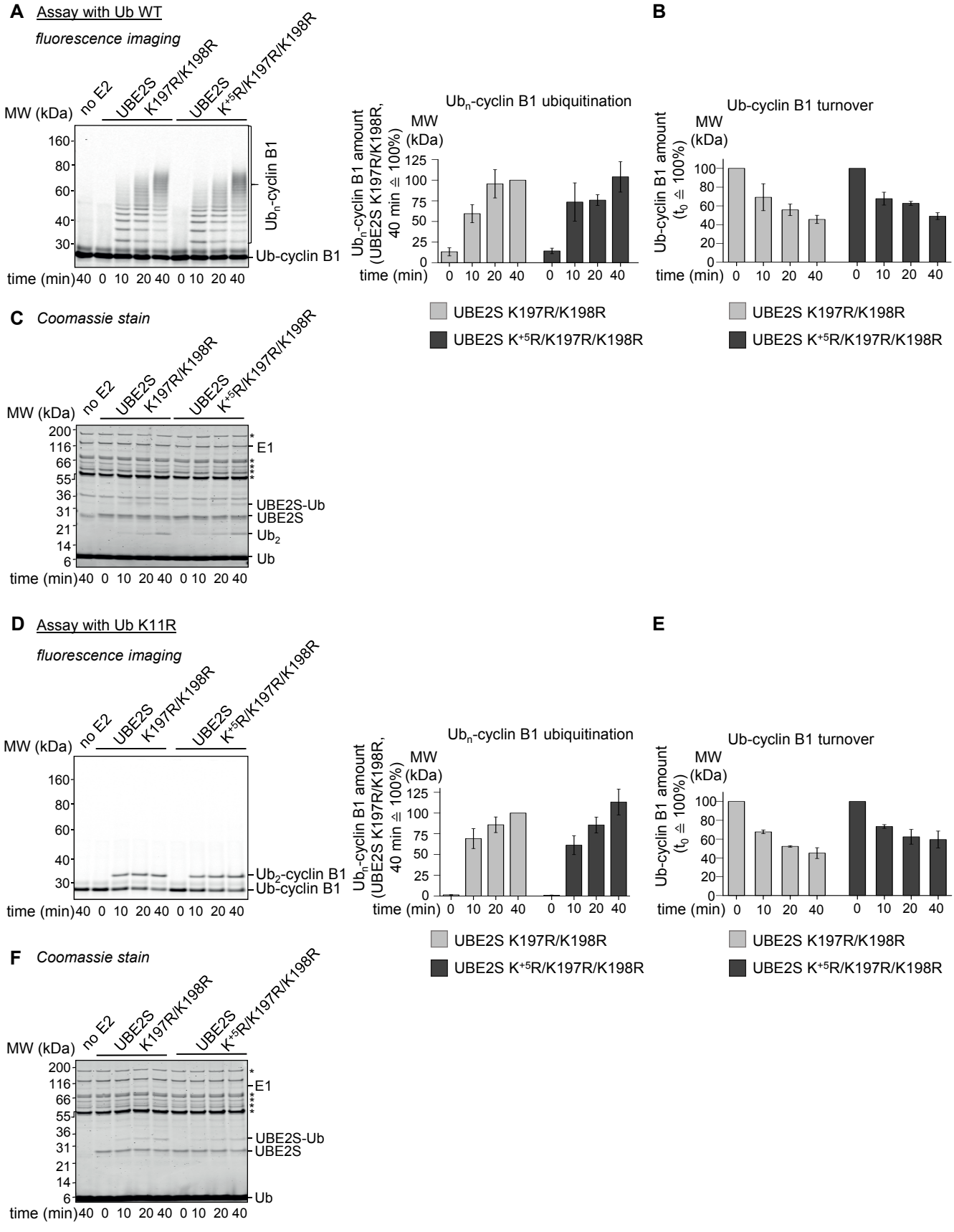
A
Assay with Ub WT
fluorescence imaging
no E2
UBE2S K197R/K198R
UBE2S K+5R/K197R/K198R
MW (kDa)
160
80
60
40
30
Ubn-cyclin B1
Ub-cyclin B1
time (min) 40 0 10 20 40 0 10 20 40
Ubn-cyclin B1 ubiquitination
Ubn-cyclin B1 amount (UBE2S K197R/K198R, 40 min ≙ 100%)
MW (kDa)
125
100
75
50
25
0
time (min) 0 10 20 40 0 10 20 40
B
Ub-cyclin B1 turnover
Ub-cyclin B1 amount (t0 ≙ 100%)
MW (kDa)
100
80
60
40
20
0
time (min) 0 10 20 40 0 10 20 40
UBE2S K197R/K198R
UBE2S K+5R/K197R/K198R
C
Coomassie stain
no E2
UBE2S K197R/K198R
UBE2S K+5R/K197R/K198R
MW (kDa)
200
116
66
55
36
31
21
14
6
E1
UBE2S-Ub
UBE2S
Ub2
Ub
time (min) 40 0 10 20 40 0 10 20 40
D
Assay with Ub K11R
fluorescence imaging
no E2
UBE2S K197R/K198R
UBE2S K+5R/K197R/K198R
MW (kDa)
160
80
60
40
30
Ub2-cyclin B1
Ub-cyclin B1
time (min) 40 0 10 20 40 0 10 20 40
Ubn-cyclin B1 ubiquitination
Ubn-cyclin B1 amount (UBE2S K197R/K198R, 40 min ≙ 100%)
MW (kDa)
125
100
75
50
25
0
time (min) 0 10 20 40 0 10 20 40
E
Ub-cyclin B1 turnover
Ub-cyclin B1 amount (t0 ≙ 100%)
MW (kDa)
100
80
60
40
20
0
time (min) 0 10 20 40 0 10 20 40
UBE2S K197R/K198R
UBE2S K+5R/K197R/K198R
F
Coomassie stain
no E2
UBE2S K197R/K198R
UBE2S K+5R/K197R/K198R
MW (kDa)
200
116
66
55
36
31
21
14
6
E1
UBE2S-Ub
UBE2S
Ub
time (min) 40 0 10 20 40 0 10 20 40

Fig S8: Impact of Lys197 and Lys198 on ubiquitin chain formation by UBE2S in APC/C-dependent reactions *in vitro (related to Fig 5C, D)*

(A) Comparison of the activities of UBE2S K197R/K198R and K^{+5}R/K197R/K198R towards a fluorophore-labeled ubiquitin-cyclin B1 fusion substrate ('Ub-cyclin B1') in the presence of recombinant APC/C and ubiquitin WT. The modification of Ub-cyclin B1 was monitored by SDS-PAGE and fluorescence imaging (left). The amount of ubiquitinated substrate at different time points was quantified, normalized to the activity of UBE2S K197R/K198R at 40 minutes (100%), and the mean and SDs from three independent experiments plotted (right). (B) Quantification of the remainder of unmodified substrate, normalized to the input amount of substrate (at t_0). (C) Coomassie-stained image of the gel shown in (A). (D) Comparison of the activities of UBE2S K197R/K198R and K^{+5}R/K197R/K198R towards a fluorophore-labeled Ub-cyclin B1 in the presence of recombinant APC/C and ubiquitin K11R. The modification of Ub-cyclin B1 was monitored by SDS-PAGE and fluorescence imaging (left). The quantification (right) was performed analogously to (A). (E) Quantification of the remainder of unmodified substrate, normalized to the input amount of substrate (at t_0). Reaction supplements and impurities are labeled with asterisks. (F) Coomassie-stained image of the gel shown in (D).

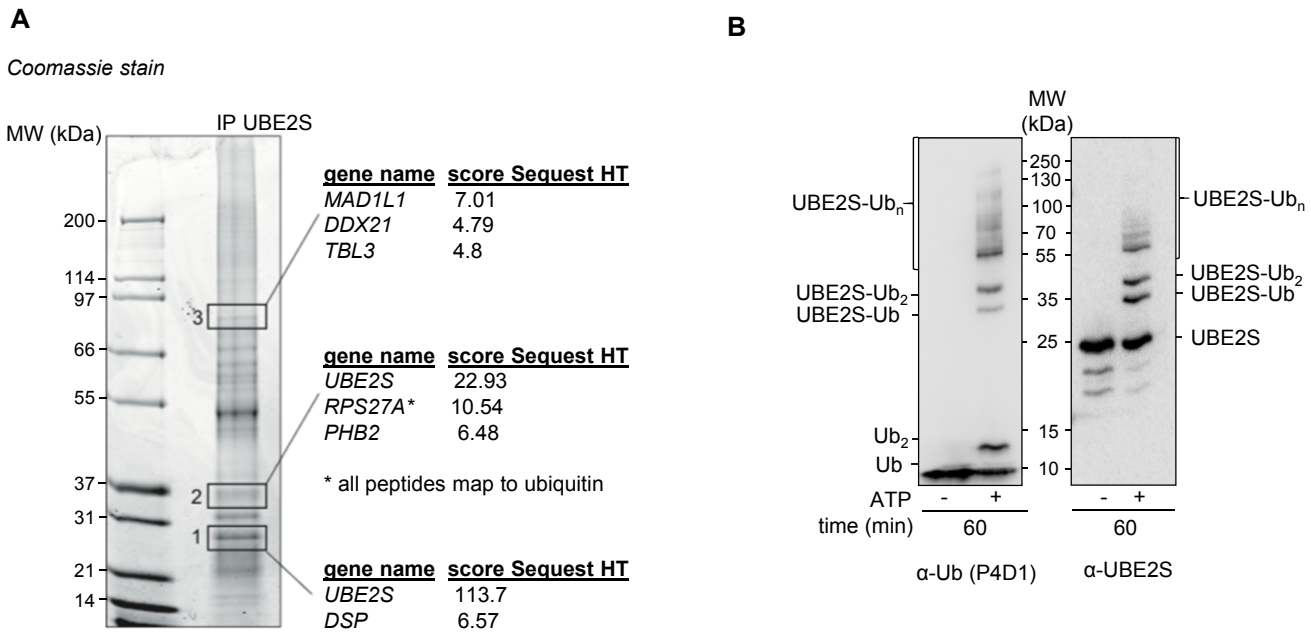

Fig S9: Characterization of the newly generated UBE2S antibody *(related to Fig 6)*
(A) UBE2S immunoprecipitation, monitored by SDS-PAGE and Coomassie staining, to identify the bands labeled as UBE2S, UBE2S-Ub, and MAD1 in Fig 6A. Bands labeled as 1, 2, and 3 were excised from the gel and analyzed by mass spectrometry (Table S2). The three top hits for each band are indicated, along with the corresponding Sequest HT scores. Note that the Western blot analysis shown in Fig 6A confirmed the identity of UBE2S and MAD1. (B) Auto-ubiquitinated UBE2S (generated in an *in vitro* reaction of 60 minutes), monitored by SDS-PAGE and Western blotting. Identical samples were blotted using a ubiquitin antibody (P4D1) (left) and the newly generated UBE2S antibody (right), respectively.

Table S1: The purified mono-ubiquitinated form of UBE2S^{UBC} has ubiquitin predominantly attached to Lys^{+5} *(related to Fig 3).*

Semi-quantitative mass spectrometric analysis of the attachment sites in the enzymatically produced, purified UBE2S^{UBC}-Ub conjugate, based on MaxQuant (Tyanova et al., 2015) (see Table 3).

Gly-Gly-Lys site detected	MS1 intensity	% of Gly-Gly-modification
68	1.43E+08	4.56
100 (= Lys^{+5})	**3.00E+09**	95.44

Table S4: Oligonucleotides used for sub-cloning and mutagenesis *(related to STAR Methods)*

REAGENT or RESOURCE	SOURCE	IDENTIFIER
Oligonucleotides		
primer $K^{+5}R$ pCCA1 fwd GATCTGCGTCAACGTGCTCCGTAGGGACTGGACGGCTGAG	this paper	N/A
primer $K^{+5}R$ pCCA1 rev CTCAGCCGTCCAGTCCCTACGGAGCACGTTGACGCAGATC	this paper	N/A
primer K197R/K198R fwd GGTCCCATGGCCCGTCGTCATGCTGGAGAAAG	this paper	N/A
primer K197R/K198R rev CTTTCTCCAGCATGACGACGGGCCATGGGACC	this paper	N/A
primer C95A fwd CCAGTGGCGAGATCGCAGTCAACGTGCTCAAG	this paper	N/A
primer C95A rev CTTGAGCACGTTGACTGCGATCTCGCCACTGG	this paper	N/A
RF primer 3HA UBE2S in pCCA1 fwd GCTCACAGAGAACAGATTGGTGGGATGTACCCATACGATGTTCCAG	this paper	N/A
RF primer 3HA UBE2S in pCCA1 rev TGATAGGCCTGCATTCGATGAGGTGCTACAGCCGCCGCAGCGC	this paper	N/A
RF primer 3HA $UBE2S^{UBC}$ in pCCA1 fwd GCTCACAGAGAACAGATTGGTGGGATGTACCCATACGATGTTCCAG	this paper	N/A
RF primer 3HA $UBE2S^{UBC}$ in pCCA1 rev TGATAGGCCTGCATTCGATGAGGTGTTATTACCCGTGGATCTCTGTGAG	this paper	N/A
primer $K^{+5}R$ wobble UBE2S fwd GTGTGAATGTCTTGAGGCGCGATTGGACCGCG	this paper	N/A
primer $K^{+5}R$ wobble UBE2S rev CGCGGTCCAATCGCGCCTCAAGACATTCACAC	this paper	N/A
primer C95S fwd	Wickliffe et al., 2011	N/A
primer C95S rev	Wickliffe et al., 2011	N/A
primer C118M fwd	Lorenz et al., 2016	N/A
primer C118M rev	Lorenz et al., 2016	N/A
primer $K^{+5}C$ with C95S fwd ATCTCCGTCAACGTGCTCTGCAGGGACTGGACGGCTGAG	this paper	N/A
primer $K^{+5}C$ with C95S rev CTCAGCCGTCCAGTCCCTGCAGAGCACGTTGACGGAGAT	this paper	N/A
primer C0 ubiquitin fwd GGAGATATACATTGCATGCAGATTTTCGTGAAAAC	this paper	N/A
primer C0 ubiquitin rev GTTTTCACGAAAATCTGCATGCAATGTATATCTCC	this paper	N/A
pCDNA5 FRT/TO-MCS-IRES2-eGFP-linear fwd AAAAAGAGCCTTAAGAAGATTATAGCCGGGATCCGCCCCTCTCCCTC	this paper	N/A
pCDNA5 FRT/TO-MCS-IRES2-eGFP-linear rev GCAAATTTTCGACATTACTATTCATCTCGGTACCAAGCTTAAGTTTAAACGC	this paper	N/A
primer UBE2S insert pCDNA5 FRT/TO-MCS-IRES2-eGFP fwd GCGTTTAAACTTAAGCTTGGTACCGAGATGAATAGTAATGTCGAAAATTTGC	this paper	N/A
primer Ube2S insert pCDNA5 FRT/TO-MCS-IRES2-eGFP rev GAGGGAGAGGGGCGGATCCCGGCTATAATCTTCTTAAGGCTCTTTTTT	this paper	N/A